Effect of Changing Iron Content and Excitation Frequency on Magnetic Particle Imaging Signal: A Comparative Study of Synomag® Nanoparticles

Kalthoum Riahi, Max T. Rietberg, Javier Perez y Perez, Corné Dijkstra, Bennie ten Haken, Lejla Alic

Abstract—Magnetic nanoparticles (MNPs) are widely used to facilitate magnetic particle imaging (MPI) which has the potential to become the leading diagnostic instrument for biomedical imaging. This comparative study assesses the effects of changing iron content and excitation frequency on point-spread function (PSF) representing the effect of magnetization reversal. PSF is quantified by features of interest for MPI: i.e., drive field amplitude and full-width-at-half-maximum (FWHM). A superparamagnetic quantifier (SPaQ) is used to assess differential magnetic susceptibility of two commercially available MNPs: Synomag®-D50 and Synomag®-D70. For both MNPs, the signal output depends on increase in drive field frequency and amount of iron-oxide, which might be hampering the sensitivity of MPI systems that perform on higher frequencies. Nevertheless, there is a clear potential of Synomag®-D for a stable MPI resolution, especially in case of 70 nm version, that is independent of either drive field frequency or amount of iron-oxide.

Keywords—Magnetic nanoparticles, MNPs, Differential magnetic susceptibility, DMS, Magnetic particle imaging, MPI, magnetic relaxation, Synomag®-D.

I. INTRODUCTION

MNPs are extensively tested for the magnetic particle imaging (MPI) for biomedical imaging technology [1]. MPI enables real-time imaging with high spatial resolution (paramount for simultaneous high sensitivity and specificity) by detecting the non-linear magnetization responses of MNPs. The most frequently used MNPs are superparamagnetic iron oxide nanoparticles (SPIONs) with a slightly different response to the applied magnetic field compared to the surrounding tissue. As illustrated in Fig. 1 (b), the shape of the PSF represents the magnetization reversal to the applied magnetic field which is governed by two distinct relaxation processes: Brownian relaxation and Néel relaxation [2]. Brownian relaxation is governed by the physical rotation of the MNP hydrodynamic volume, whereas Néel relaxation refers to the fluctuation of magnetic moment ruled by the magnetic core of an MNP. As illustrated in Fig. 1 (a), the dominant relaxation mechanism depends primarily on the MNP size [3] with a clear range in iron-core sizes (15-25 nm) where the influence of both Brownian and Néel are relevant. Similarly, Tay et al. discovered that MPI resolution follows the steady-state prediction, i.e. improves with increasing

Kalthoum Riahi*, Max T. Rietberg, Javier Perez y Perez, Corné Dijkstra, Bennie ten Haken, and Lejla Alic are with the Magnetic Detection and Imaging group, Technical Medical Centre University of Twente, the Netherlands (*corresponding author, e-mail: kalthoumriahi@gmail.com).

magnetic core size up to approximately 25 nm where Brownian relaxation becomes leading [4]. MNP with a core size larger than 25 nm experience increased drag, slowing their magnetization response and limiting MPI resolution [5].

The sensitivity and resolution of MPI systems is driven primarily by the shape of PSF for each specific nanoparticle; i.e., drive field amplitude is responsible for the sensitivity and FHWM is responsible for the resolution. Therefore, this study compares plain Synomag®-D nanoparticles (Micromod Partikeltechnologie GmbH, Germany) in terms of their potential as MPI tracer in terms of drive field amplitude and FWHM.

II. MATERIALS AND METHODS

A. Magnetic Nanoparticles

A series of samples containing Synomag®-D nanoparticles with different nanoflower sizes were used in this study: i.e., 50 nm (0.1×10^{12} particles per mg) and 70 nm (2.2×10^{12} particles per mg). The plain Synomag®-D nanoflowers are dextran coated iron oxide nanoparticles (mixture of $\gamma-Fe_2O_3$ and Fe_3O_4) synthesized by a polyol method [6]. For both Synomag®-D nanoflowers, series of four samples containing 20 µg, 0 µg, 100 µg and 140 µg iron-oxide in a total volume of 140 µl were diluted in water.

B. TEM

A 2 µl droplet of SPION was released onto a carbon film coated and perforated copper grid. The droplet was dried at room temperature for 12 hours, after being ultra-sonicated for 10 min to reduce aggregation of the particles and to achieve an equal particle distribution. The core sizes and shapes of MNPs were observed directly via TEM (Philips CM300ST-FEG), using an electron acceleration voltage of 300 kV at a point resolution of 0.2 nm at 300 kV and a line resolution of 0.14 nm at 300 kV. The 12-bit TEM images (with a resolution of 2048 x 2048 pixels) were analyzed semi-quantitatively using an in-house developed software (MATLAB environment Version 9.0. MathWorks, Inc., Natick, Massachusetts, USA) to calculate an average core size for both samples [7].

C. SPaQ

The magnetic properties of the samples were characterized using SPaQ which is a custom differential susceptometry device used to measure the magnetization response of nanoparticles to an applied alternating magnetic field [8]. The SPaQ combines a low-amplitude alternating magnetic field

World Academy of Science, Engineering and Technology
International Journal of Chemical and Materials Engineering
Vol:15, No:5, 2021

with a gradual DC offset field to measure the dynamic magnetization curve [9]. An alternating field magnitude of 1.33 mT was ramped with an offset field (swept between −13.3 and +13.3 mT) in 1 s. The excitation frequency was set to 2.5 kHz, 5 kHz and 7 kHz. The sample temperature during these measurements was maintained at 20 °C.
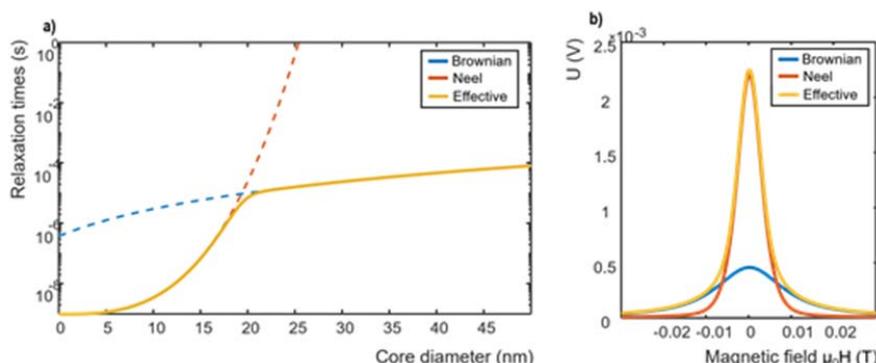
Fig. 1 (a) Individual components of relaxation as a function of core diameter and (b) the corresponding PRF
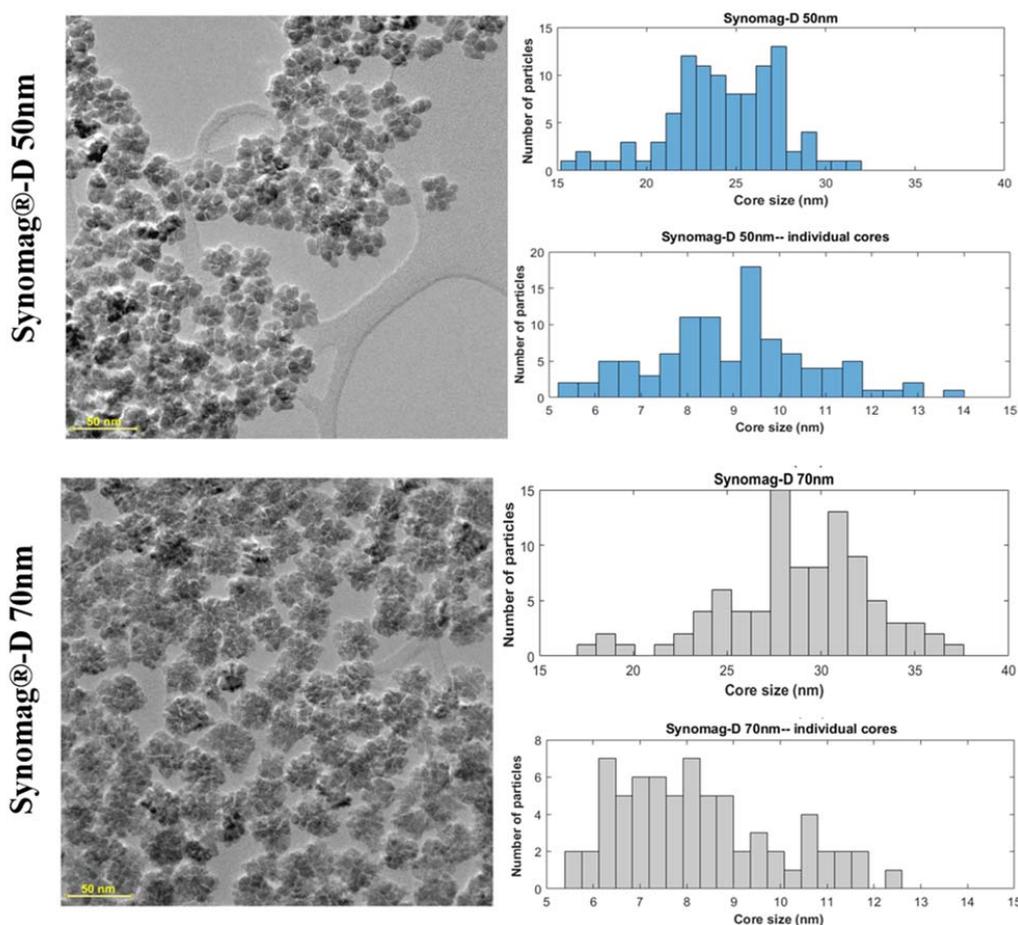

Fig. 2 TEM micrographs of Synomag®-D nanoparticles (50 nm hydrodynamic size-first row, and 70 nm hydrodynamic size -second row). The corresponding histograms illustrate individual core size and total iron-oxide size

III. RESULT

The magnetic cores for both Synomag®-D nanoparticles can be observed from transmission electron micrographs, since their electron density is higher than that of the surrounding polymer coating. TEM images of clear nanoflower shape are shown in Fig. 2, with each assembly of a nanoflower containing multiple individual nano cores in densely clustered aggregates of iron oxides. As illustrated in histograms in Fig. 2, there was no significant difference in individual core sizes between the two Synomag®-D MNPs: i.e., 9 nm for Synomag®-D50 sample and 8.25 nm for Synomag ®-D70 sample. The average size of entire

World Academy of Science, Engineering and Technology
International Journal of Chemical and Materials Engineering
Vol:15, No:5, 2021

nanoflower was 24 nm and 29 nm for Synomag®-D50 and Synomag®-D70, respectively. This observation indicates that

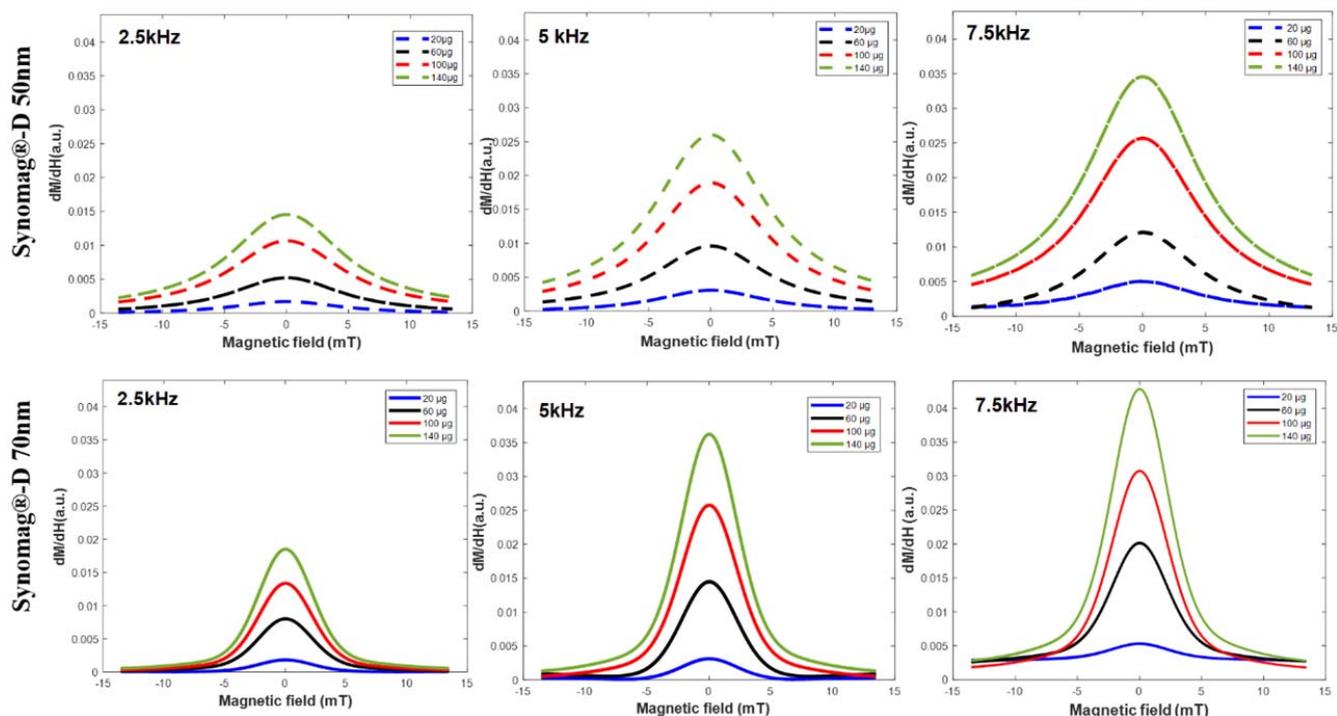the size of coating around Synomag®-D70 is larger than Synomag®-D50.

Fig. 3 PSF for different iron contents measured under different expiation frequencies for Synomag®-D50 and Synomag®-D70
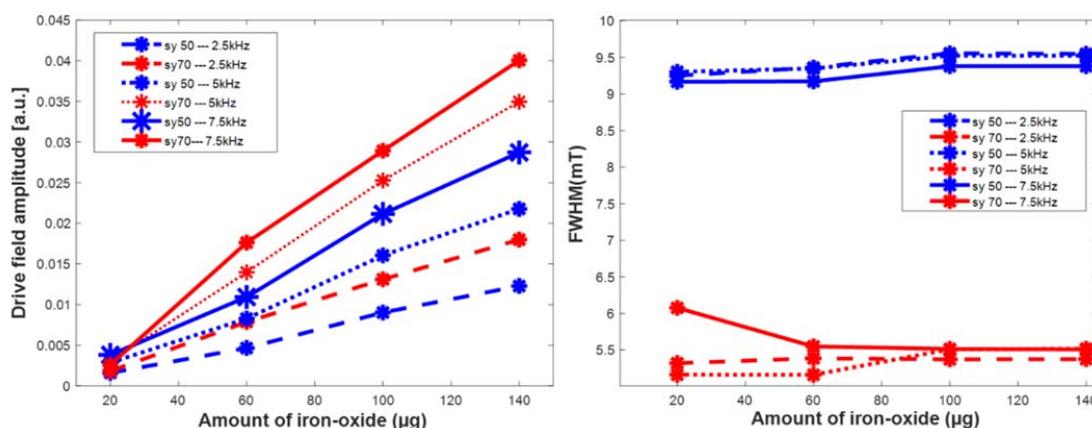

Fig. 4 Drive field amplitude and FWHM as a function of iron-oxide mass

The differential magnetic susceptibility for both types of Synomag ®-D with different iron content is measured at three different excitation frequencies: 2.5 kHz, 5 kHz and 7.5 kHz. The resulting changes in the differential magnetic susceptibility PSF as illustrated in Fig. 3. Synomag®-D50 has a larger FWHM at the same amount of iron oxide. The amplitude of the PSF signal increases with the increasing amount of iron oxide and with the increase of the excitation frequency.

The influence of increasing amount of iron content in nanoflower samples is illustrated in Fig. 4. For both nanoflowers, the drive field amplitude linearly increases with the amount of iron-oxide for both particles with a slightly

steeper incline for Synomag®-D70. Higher excitation frequency caused increased slope even more. In terms of FWHM, both nanoflowers are reasonably steady as a function of excitation frequency and are independent of amount of MNPs. The FWHM of Synomag®-D50 is significantly higher (nearly double) than FWHM of Synomag®-D70.

Fig. 5 illustrates the comparison between Synomag®-D50 and Synomag®-D70 for different field frequencies in terms of drive field amplitude and FWHM. The amplitude change for the increasing frequency of the excitation field is relatively low for the low iron-content samples. The dependency of the excitation frequency is more prominent for samples containing more iron-oxide. In terms of FWHM, both nanoflower MNPs

World Academy of Science, Engineering and Technology
International Journal of Chemical and Materials Engineering
Vol:15, No:5, 2021

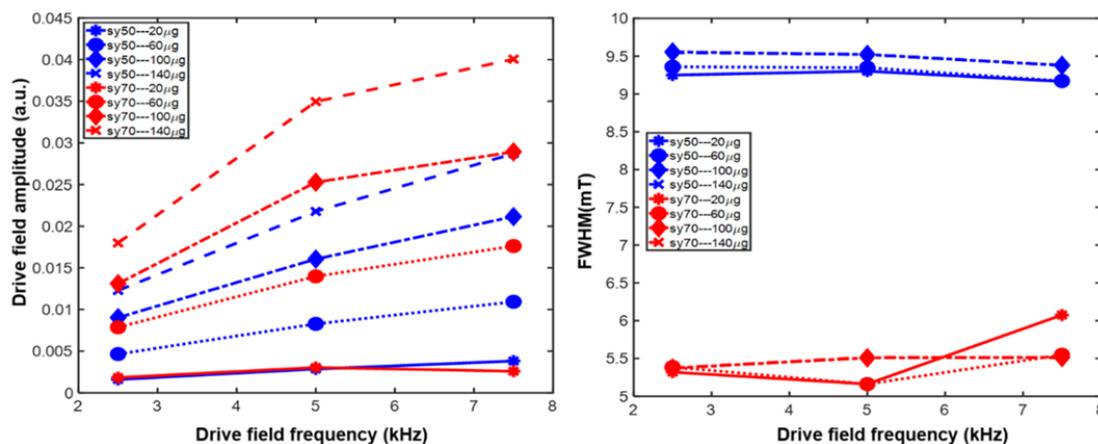are steady and not changing significantly for increasing excitation frequency.

Fig. 5 Comparison between Synomag®-D50 and Synomag®-D70 for different field frequencies in terms of drive field amplitude and FWHM

In conclusion, both particles show promising potential as MPI tracer. The signal output depends on both increase in drive field frequency and amount of iron-oxide. The latter one might be hampering the sensitivity of MPI systems perform on higher frequencies in a low iron content use cases. There is a clear advantage of Synomag®-D, especially in case of 70 nm version, illustrated in a stable resolution independent of either drive field frequency or amount of iron-oxide.

REFERENCES

[1] E. Teeman, C. Shasha, J. E. Evans, and K. M. Krishnan, "Intracellular dynamics of superparamagnetic iron oxide nanoparticles for magnetic particle imaging," *Nanoscale*, 2019.
[2] S. A. Shah, D. B. Reeves, R. M. Ferguson, J. B. Weaver, and K. M. Krishnan, "Mixed Brownian alignment and Néel rotations in superparamagnetic iron oxide nanoparticle suspensions driven by an ac field," *Phys. Rev. B - Condens. Matter Mater. Phys.*, 2015.
[3] F. Ludwig *et al.*, "Characterization of magnetic nanoparticle systems with respect to their magnetic particle imaging performance," *Biomedizinische Technik*. 2013.
[4] Z. W. Tay, D. W. Hensley, E. C. Vreeland, B. Zheng, and S. M. Conolly, "The relaxation wall: experimental limits to improving MPI spatial resolution by increasing nanoparticle core size," *Biomed. Phys. Eng. Express*, 2017.
[5] P. J. Sehl, O.C.; Gevaert, J.J.; Melo, K.P.; Knier, N.N.; Foster, "A Perspective on Cell Tracking with Magnetic Particle Imaging."
[6] L. Lartigue *et al.*, "Cooperative organization in iron oxide multi-core nanoparticles potentiates their efficiency as heating mediators and MRI contrast agents," *ACS Nano*, 2012.
[7] K. Riahi, M. M. van de Loosdrecht, L. Alic, and B. ten Haken, "Assessment of differential magnetic susceptibility in nanoparticles: Effects of changes in viscosity and immobilisation," *J. Magn. Magn. Mater.*, 2020.
[8] M. M. Van De Loosdrecht *et al.*, "A novel characterization technique for superparamagnetic iron oxide nanoparticles: The superparamagnetic quantifier, compared with magnetic particle spectroscopy," *Rev. Sci. Instrum.*, vol. 90, no. 2, Feb. 2019.
[9] K. Riahi, M. M. van de Loosdrecht, L. Alic, and B. Ten Haken, "Magnetic performance of synomag nanoparticles in various environments," *Int. J. Magn. Part. Imaging*, 2020.